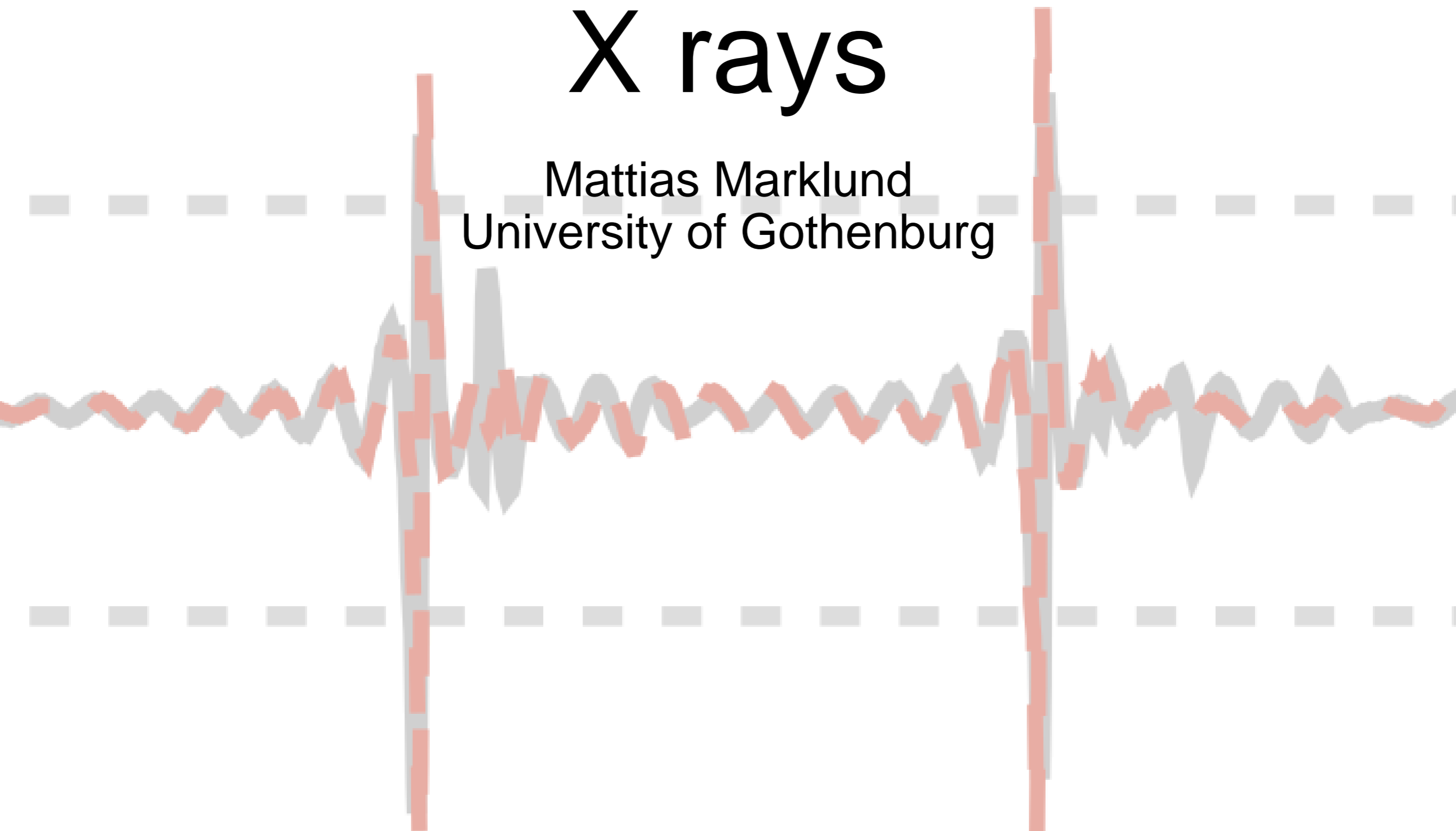


Nonlinear physics with X rays

Mattias Marklund
University of Gothenburg



Outline

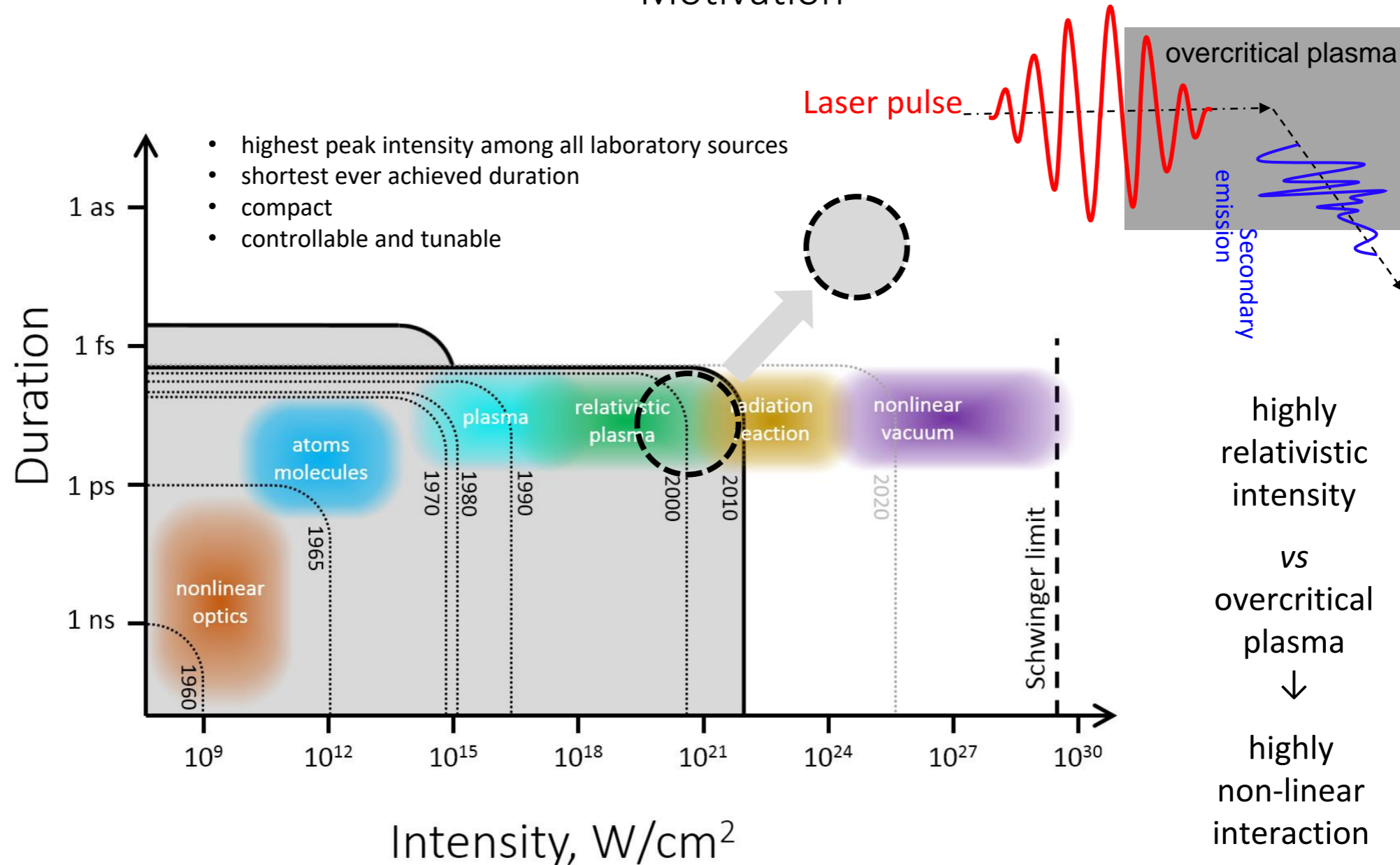
- Parameters
- Relativistically intense X-rays
- Examples of nonlinear problems
- Conclusions

Parameters

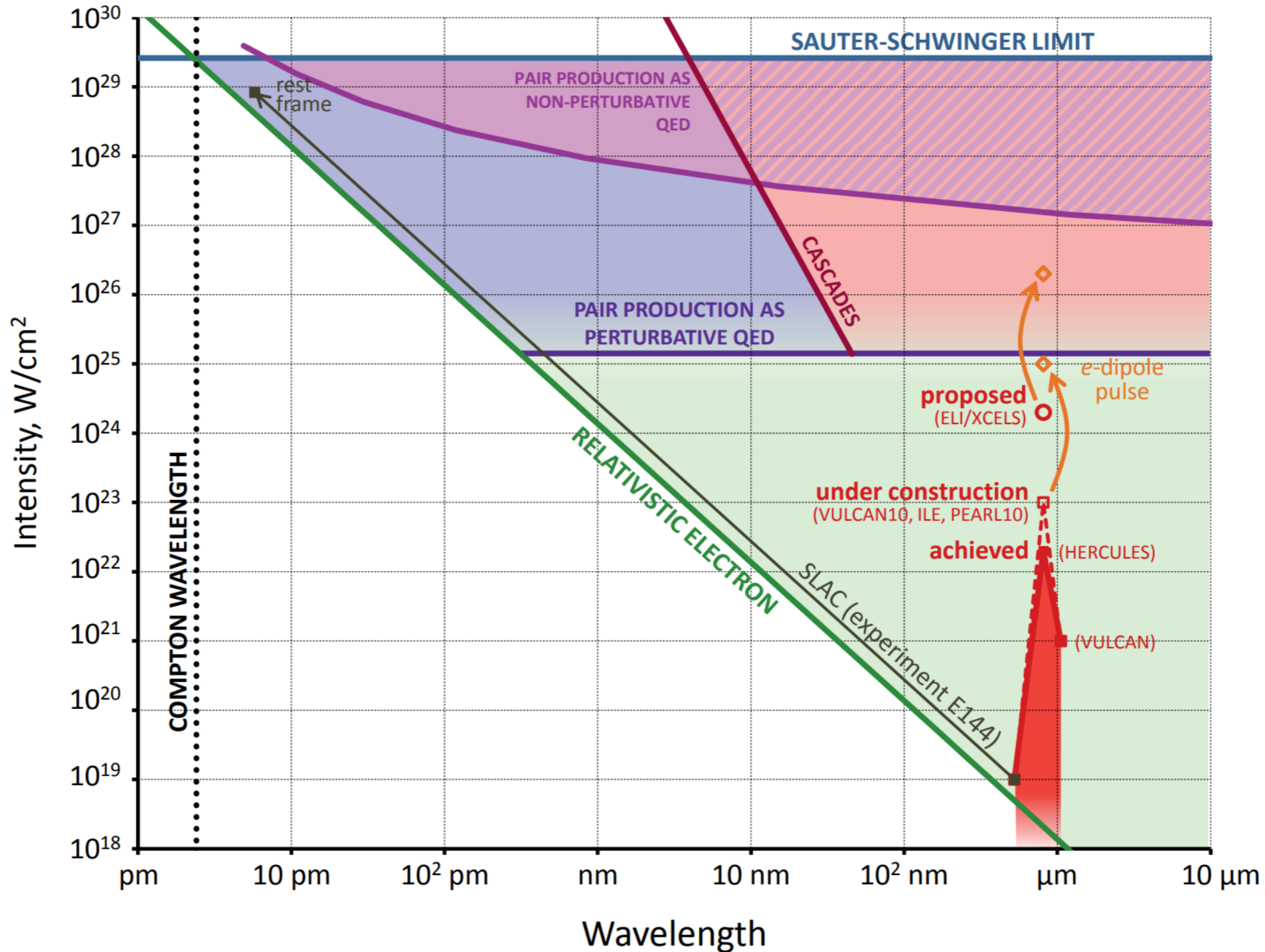
- The Schwinger critical field: $E_{\text{crit}} = \frac{m^2 c^3}{e\hbar}$
- Field invariants: $\mathcal{F}^2 = \frac{E^2 - c^2 B^2}{E_{\text{crit}}^2}$ $\mathcal{G}^2 = \frac{c\mathbf{E} \cdot \mathbf{B}}{E_{\text{crit}}^2}$
- Quantum nonlinearity parameters:
$$\chi_e = \frac{\gamma \sqrt{(\mathbf{E} + \mathbf{v} \times \mathbf{B})^2 - (\mathbf{E} \cdot \mathbf{v}/c)^2}}{E_{\text{crit}}}$$
$$\chi_\gamma = \frac{\hbar\omega}{mc^2} \frac{\sqrt{(\mathbf{E} + \mathbf{n} \times c\mathbf{B})^2 - (\mathbf{E} \cdot \mathbf{n})^2}}{E_{\text{crit}}}$$
- The normalized vector potential: $a_0 = \frac{eE_0}{mc\omega_0}$

Relativistically intense X-rays

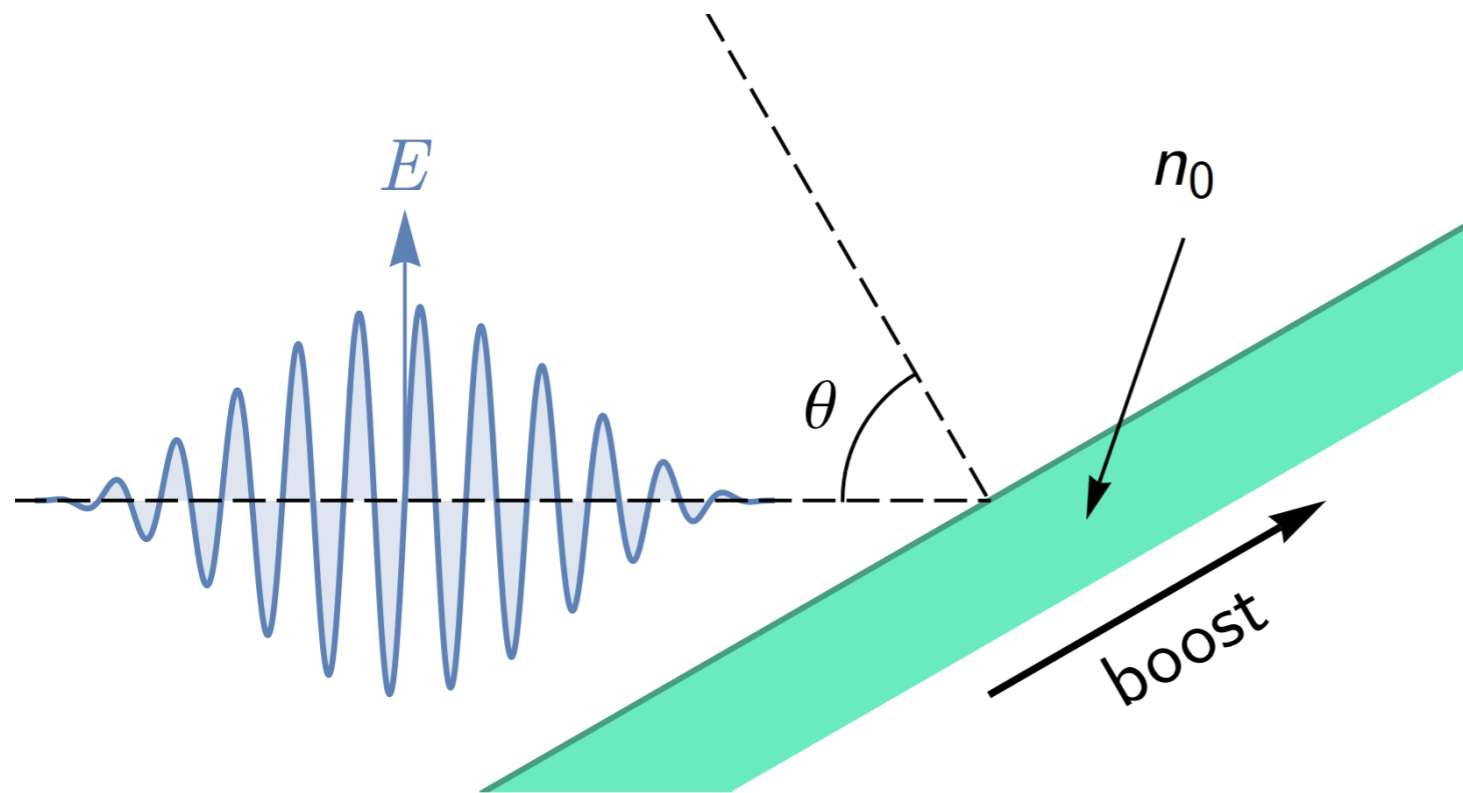
Motivation



Relativistically intense X-rays



Theoretical foundations



Plasma illuminated by laser light at oblique incidence (angle θ) can be modelled in 1D by boosting parallel to the plasma surface by $c \sin \theta$.

A. Bourdier, Phys. Fluids 26, 1804 (1983).

Under the radiation pressure the plasma forms an oscillating reflecting interface.

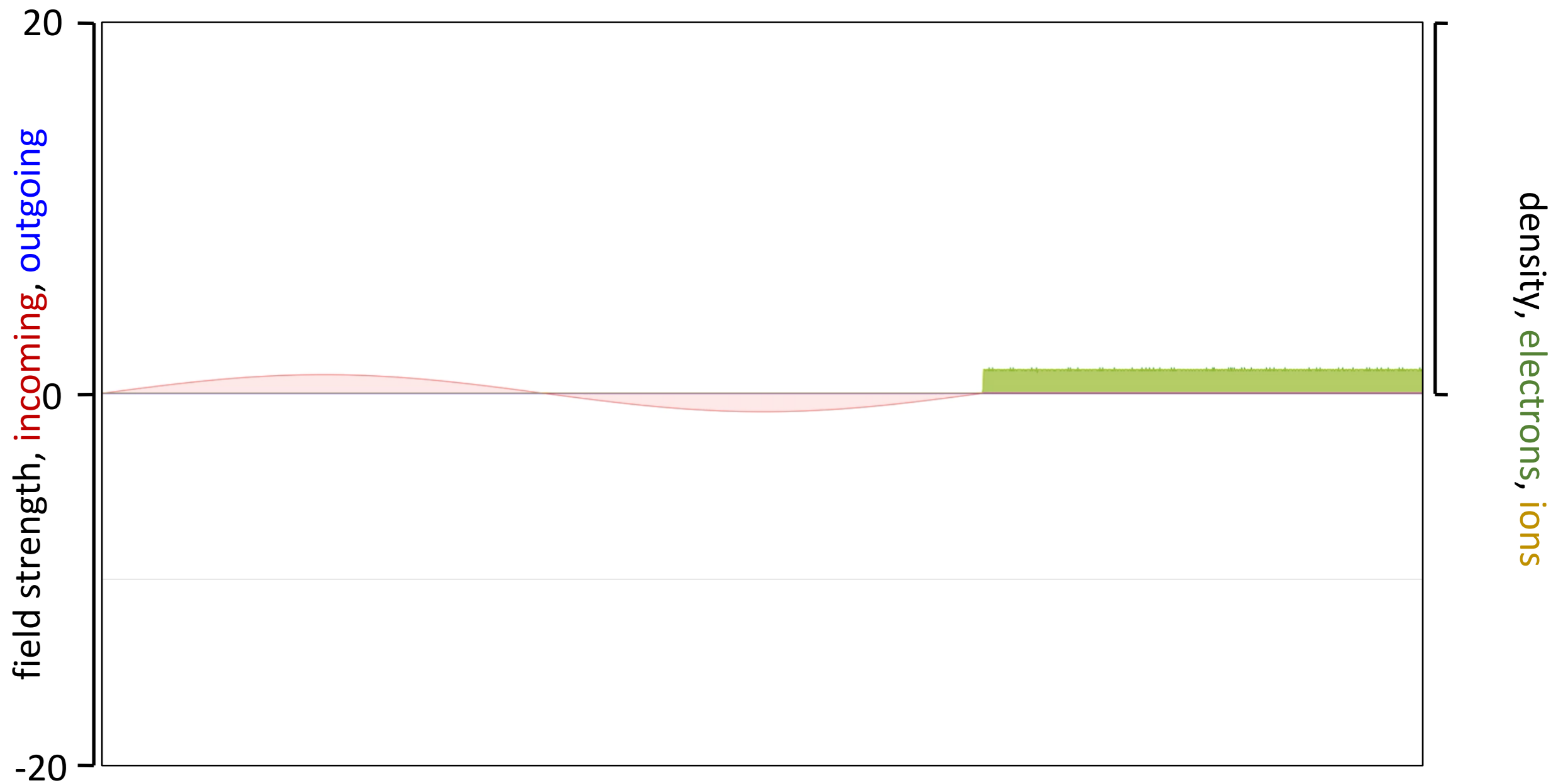
Bulanov *et al.* Phys. Plasmas 1, 745 (1994);
Lichters *et al.* Phys. Plasmas 3, 3425 (1996).

The scenario is determined by the relativistic similarity parameter $S = n/a$.

S. Gordienko *et al.* PRL 93, 115002 (2004).

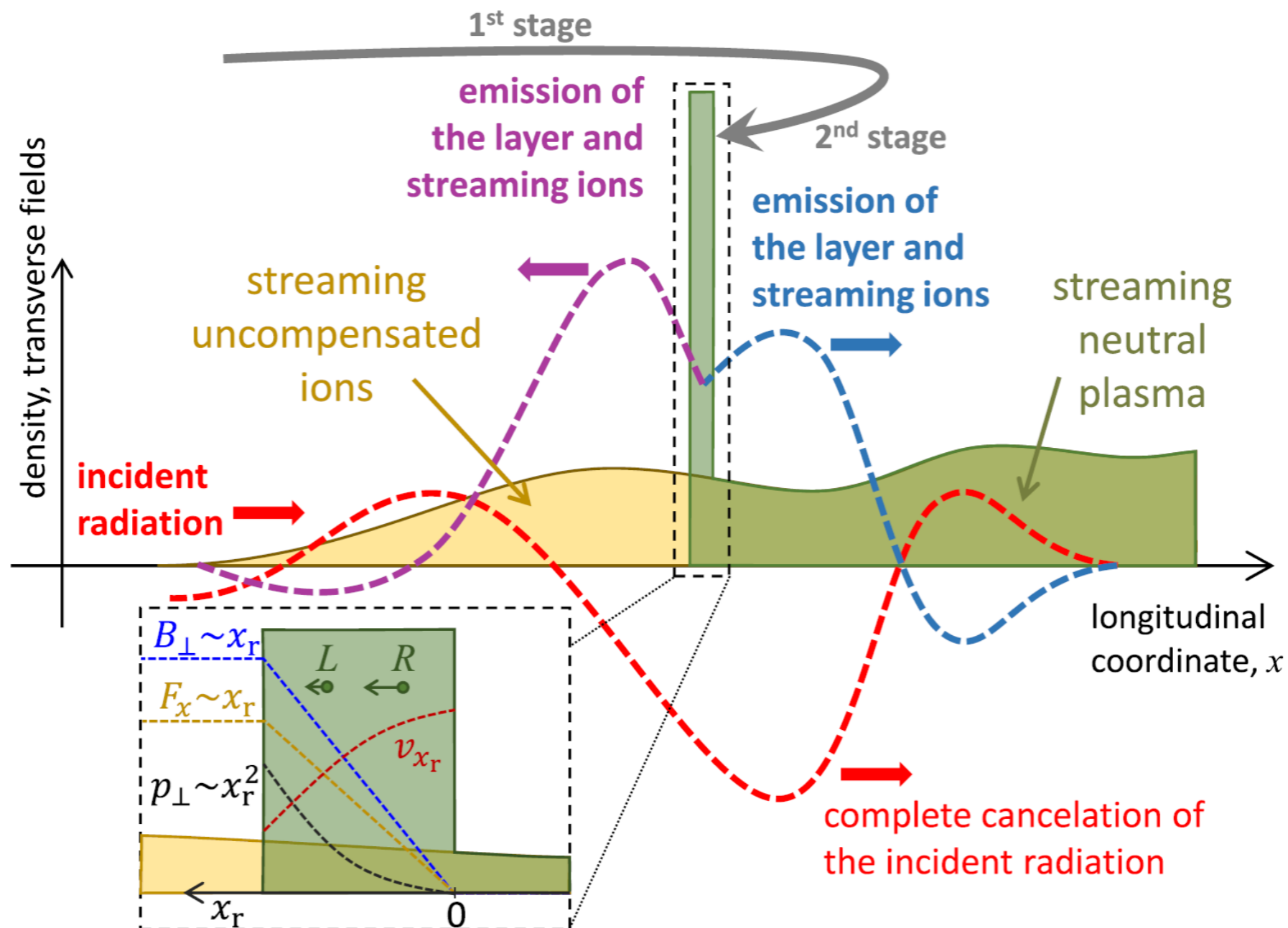
Optimizing the signal

The “dream regime” of laser-plasma interaction

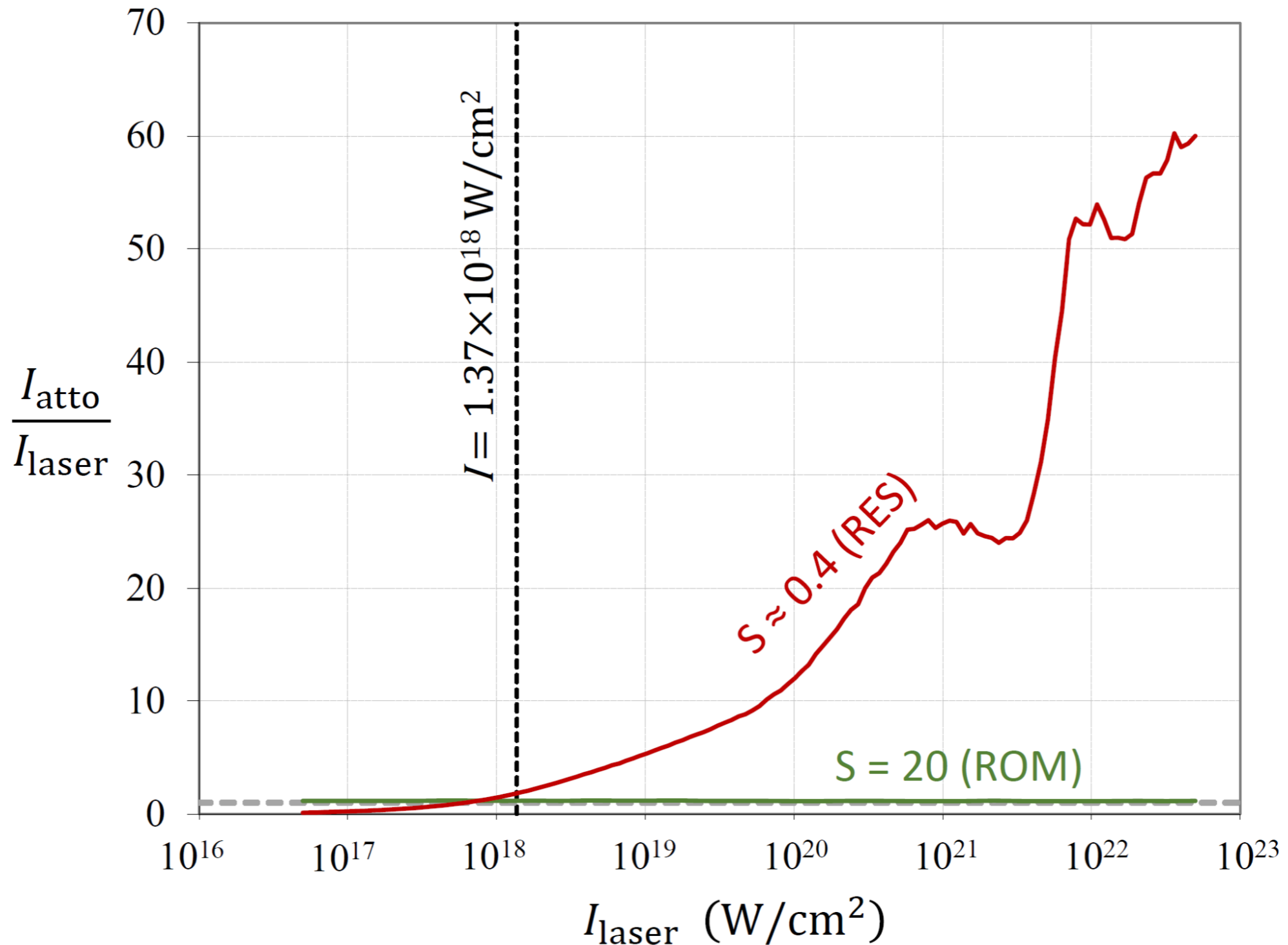


The relativistic electron spring: Gonoskov *et al.* PRE 84, 046403 (2011)

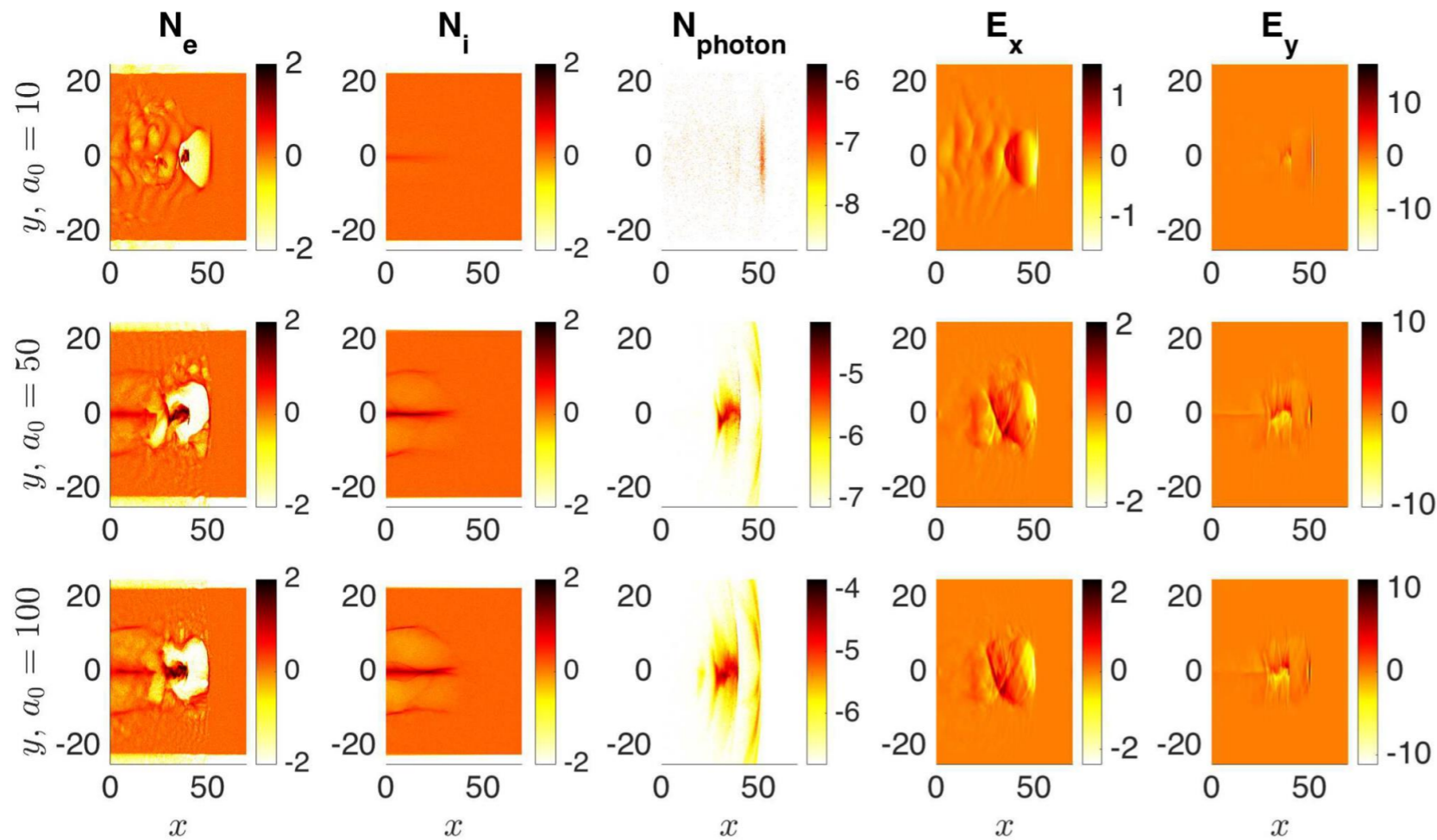
Principles of the X-ray generation



Amplifying the intensity



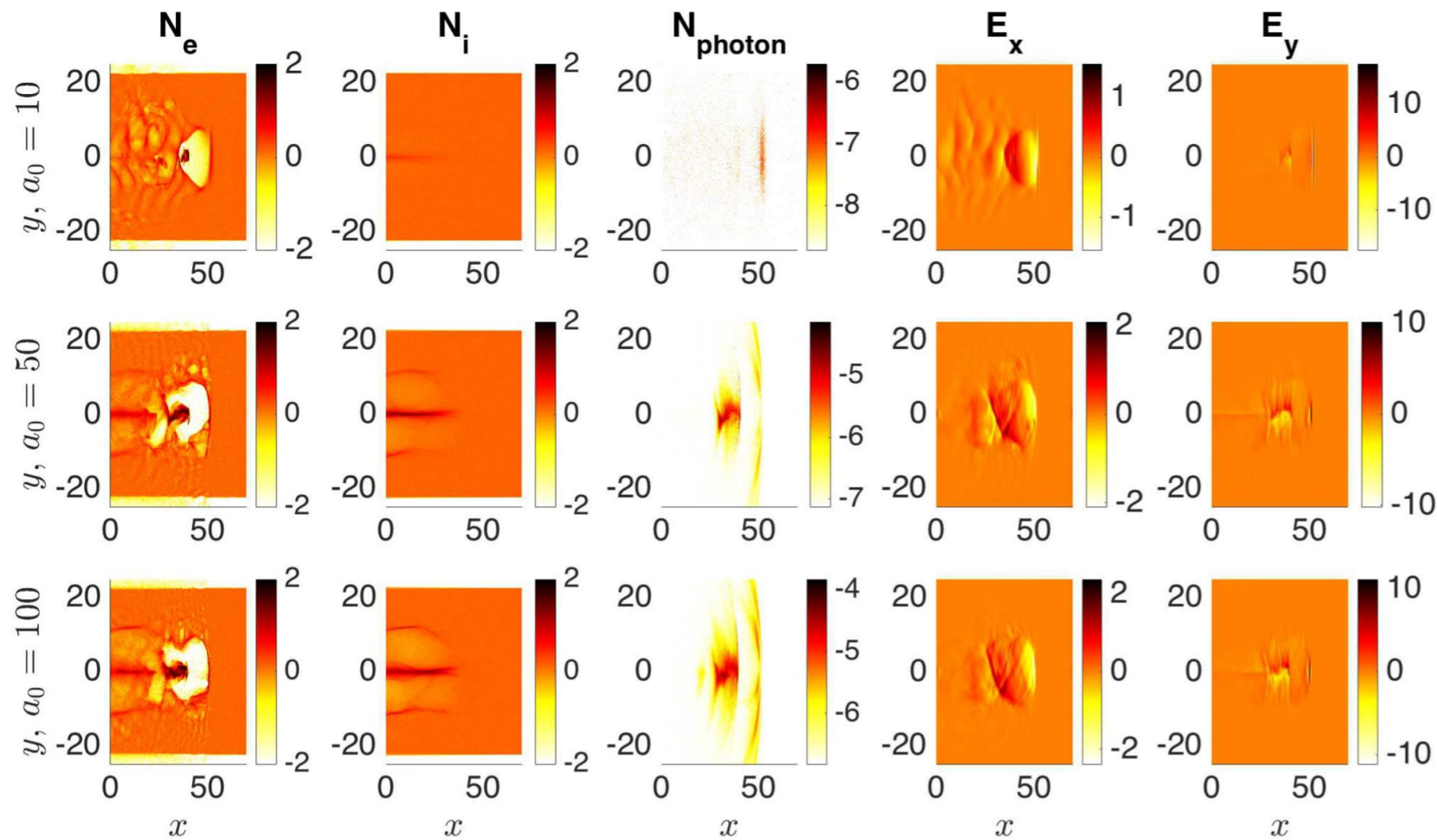
Wakefields in solids



Quantity	Scaling
Timescale	λ
Spatial dimensions of cavity	λ
Density	a_0/λ^2
Current density	a_0/λ^2
Current	a_0
Trapped charge	λa_0
Electron energy	a_0
Electromagnetic fields	a_0/λ
Pulse energy	λa_0^2
Ion motion	a_0
Quantum parameter, χ	a_0^2/λ
Radiated energy fraction	$\lambda^{1-\alpha} a_0^{2\alpha-1}$
Photon energy ($\chi \ll 1$)	a_0^3/λ
Photon energy ($\chi \sim 1$)	a_0
Time between emissions ($\chi \ll 1$)	T/a_0
Time between emissions ($\chi \sim 1$)	$T/(\lambda a_0)^{1/3}$

PIC simulations for $\lambda = 5$ nm, $S = 10^{-3}$ indicate the possibility of driving wake-fields in solids.

Wakefields in solids



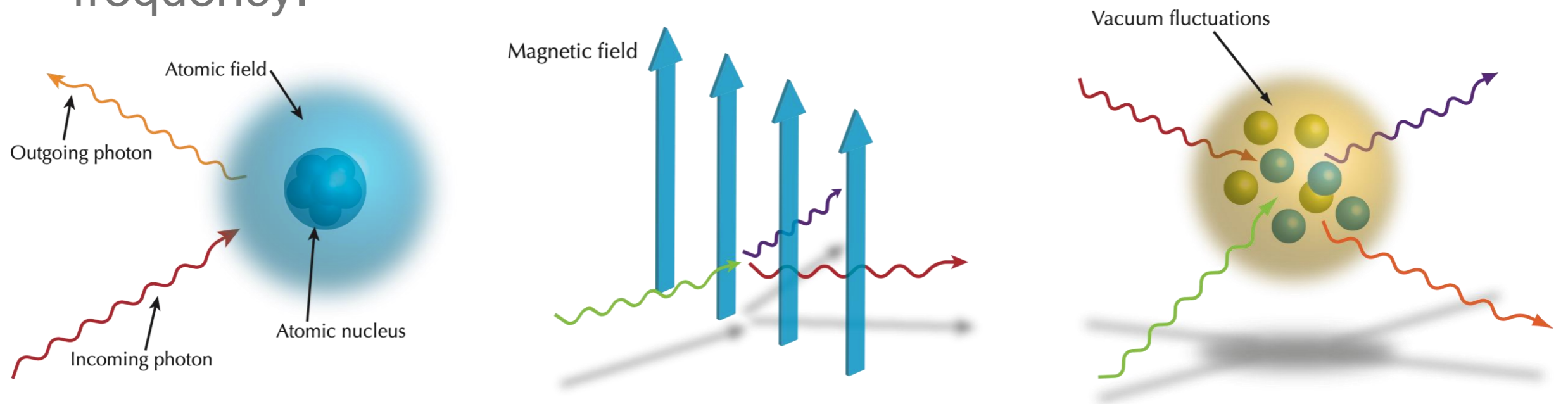
PIC simulations for $\lambda = 5$ nm, $S = 10^{-3}$ indicate the possibility of driving wake-fields in solids.

We see a possibility to significantly increase the current density, which could be important for some applications.

Quantity	Scaling
Timescale	λ
Spatial dimensions of cavity	λ
Density	a_0/λ^2
Current density	a_0/λ^2
Current	a_0
Trapped charge	λa_0
Electron energy	a_0
Electromagnetic fields	a_0/λ
Pulse energy	λa_0^2
Ion motion	a_0
Quantum parameter, χ	a_0^2/λ
Radiated energy fraction	$\lambda^{1-\alpha} a_0^{2\alpha-1}$
Photon energy ($\chi \ll 1$)	a_0^3/λ
Photon energy ($\chi \sim 1$)	a_0
Time between emissions ($\chi \ll 1$)	T/a_0
Time between emissions ($\chi \sim 1$)	$T/(\lambda a_0)^{1/3}$

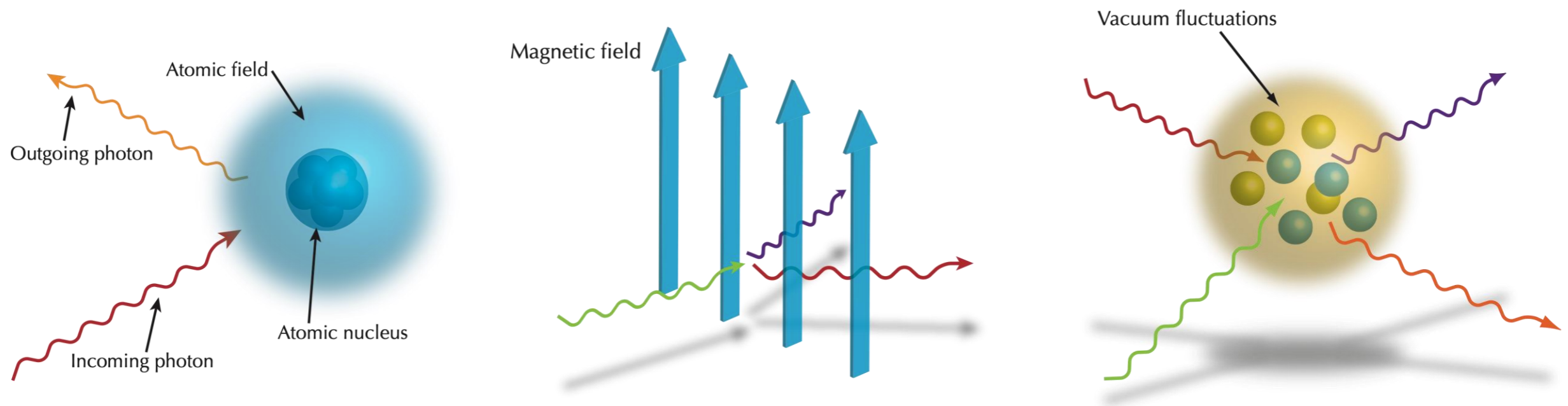
The quantum vacuum

- Photons can effectively interact via fluctuating electron-positron pairs.
- Astrophysical applications; laboratory tests of high field QED.
- Many of these crosssections scale positively with increased frequency.



The quantum vacuum

Quantity	$\chi \ll 1$	$\chi \gg 1$
photon emission rate [c/λ]	$1.44\alpha\gamma^{-1}\chi$	$1.46\alpha\gamma^{-1}\chi^{2/3}$
radiation power [mc^3/λ]	$2\alpha\chi^2/3$	$0.37\alpha\chi^{2/3}$
mean photon energy [mc^2]	$0.43\gamma\chi$	0.25γ
r.m.s. divergence angle	$1.1\gamma^{-1}$	$1.3\gamma^{-1}\chi^{1/3}$
pair creation rate [c/λ]	$0.23\alpha\gamma^{-1}\chi e^{-8/(3\chi)}$	$0.38\alpha\gamma^{-1}\chi^{2/3}$
helicity flip rate [c/λ]	$\chi^2\gamma^{-1}$	—
radiation length L_i [λ]	$33a_0^{-1}\chi^{-1}$	$55a_0^{-1}\chi^{1/3}$
mean free path L_q [λ]	$48a_0^{-1}$	$15a_0^{-1}\chi^{1/3}$
formation length L_f [λ]	$0.18a_0^{-1}$	$0.21a_0^{-1}\chi^{1/3}$
pair creation length L_p [λ]	$95a_0^{-1}e^{8/(3\chi)}$	$57a_0^{-1}\chi^{1/3}$

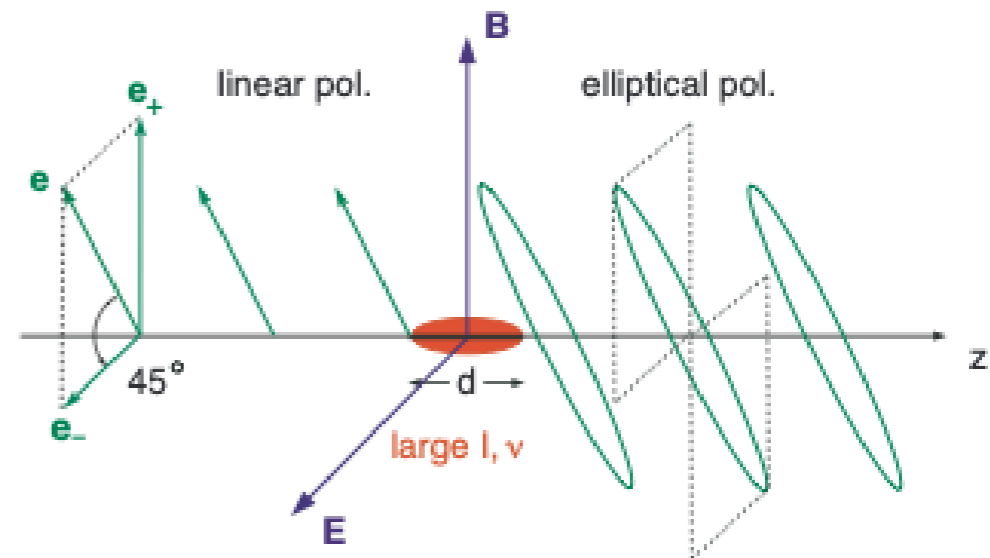


Vacuum birefringence

- The "vacuum" state (i.e. with a background field) shows a birefringent nature: an anisotropic dispersion of photons. (Adler 1970, 1971, Heyl & Hernquist 1997, Dittrich & Gies 1998, Rikken & Rizzo 2000, 2003).

$$\epsilon_{ij} = \delta_{ij} + \frac{4\alpha}{90\pi} \frac{B^2}{E_{\text{crit}}^2} \left(-\delta_{ij} + \frac{7}{2} b_i b_j \right)$$

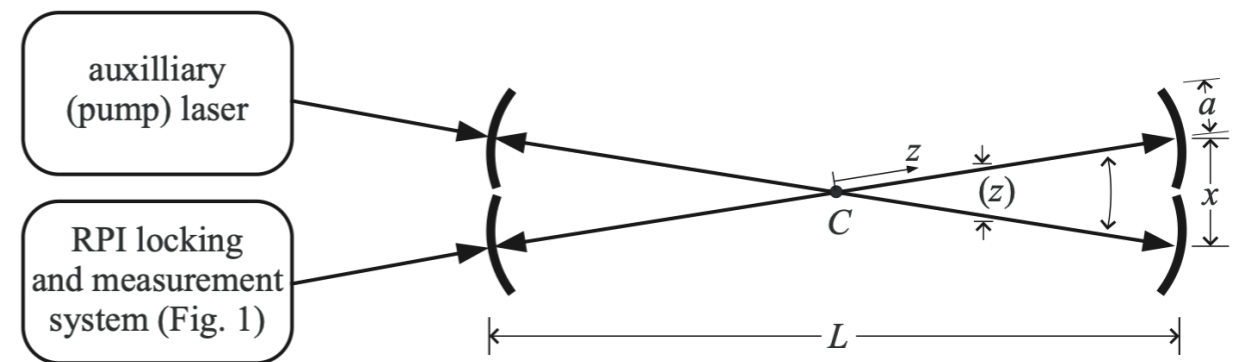
$$\mu_{ij} = \delta_{ij} + \frac{4\alpha}{90\pi} \frac{B^2}{E_{\text{crit}}^2} (\delta_{ij} + 2b_i b_j)$$



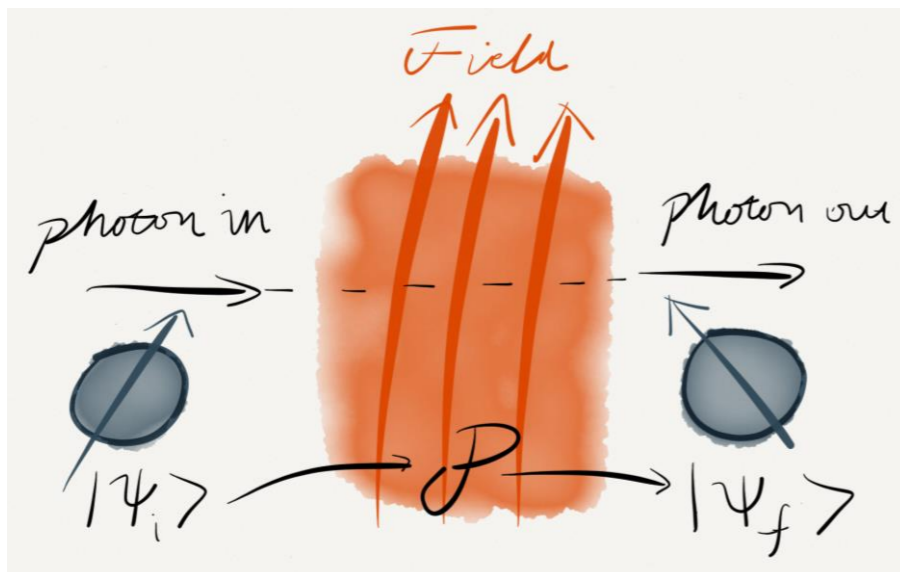
Vacuum birefringence

- Refractive index different for different propagation angles, relative external field.

$$n - 1 \sim \frac{\alpha}{90\pi} \frac{B^2}{E_{\text{crit}}^2} \sin^2 \theta$$



- Corresponds to helicity flip in QED.



Conclusions

- Strong fields should be characterized by invariant parameters.
- Relativistically intense X-rays access unexplored regions of parameter space.
- Driving wakefields in solid-density plasmas gives nanoscale/attosecond electron bunches.
- Quantum effects, such as vacuum birefringence, have strong frequency dependence. Can be tuned to processes of interest.